HHS Public Access

Author manuscript

Dev Dyn. Author manuscript; available in PMC 2023 September 18.

Published in final edited form as:

Dev Dyn. 2022 May ; 251(5): 877–884. doi:10.1002/dvdy.435.

Inactivation of *Fgf3* and *Fgf4* within the *Fgf3/Fgf4/Fgf15* gene cluster reveals their redundant requirement for mouse inner ear induction and embryonic survival

Laura Zelarayan[1,2,3,4], **Victor Vendrell**[4], **Elena Domínguez-Frutos**[4], **Iris López-Hernández**[4], **Kiril Schimmang-Alonso**[4], **María Teresa Alonso**[4], **Yolanda Alvarez**[4], **Hannes Maier**[5], **Matthew J. Anderson**[6], **Mark Lewandoski**[6], **Thomas Schimmang**[4]

[1]Institute of Pharmacology and Toxicology, University Medical Center Goettingen (UMG), Goettingen, Germany

[2]DZHK (German Center for Cardiovascular Research), partner site Goettingen, Germany

[3]Cluster of Excellence “Multiscale Bioimaging: from Molecular Machines to Networks of Excitable Cells” (MBExC), University of Goettingen, Germany

[4]Unidad de Excelencia, Instituto de Biología y Genética Molecular, Universidad de Valladolid y Consejo Superior de Investigaciones Científicas, Valladolid, Spain

[5]Department of Otorhinolaryngology, Hannover Medical School, Hannover, Germany

[6]Genetics of Vertebrate Development Section, Cancer and Developmental Biology Laboratory, National Cancer Institute, National Institutes of Health, Frederick, Maryland, USA

Abstract

Background: Fibroblast growth factors (Fgfs) are required for survival and organ formation during embryogenesis. Fgfs often execute their functions redundantly. Previous analysis of *Fgf3* mutants revealed effects on inner ear formation and embryonic survival with incomplete penetrance.

Results: Here, we show that presence of a *neomycin* resistance gene (*neo*) replacing the *Fgf3* coding region leads to reduced survival during embryogenesis and an increased penetrance of inner ear defects. $Fgf3^{neo/neo}$ mutants showed reduced expression of *Fgf4*, which is positioned in close proximity to the *Fgf3* locus in the mouse genome. Conditional inactivation of *Fgf4* during inner ear development on a *Fgf3* null background using *Fgf3/4 cis mice* revealed a redundant

Correspondence: Thomas Schimmang, Instituto de Biología y Genética Molecular, Universidad de Valladolid y Consejo Superior de Investigaciones Científicas, C/Sanz y Forés 3, E-47003 Valladolid, Spain. schimman@ibgm.uva.es.

AUTHOR CONTRIBUTIONS

Laura Zelarayan: Formal analysis (equal); investigation (equal); validation (equal); visualization (equal). **Victor Vendrell:** Formal analysis (equal); investigation (equal); visualization (equal). **Elena Dominguez-Frutos:** Formal analysis (equal); investigation (equal); validation (equal). **Iris Lopez-Hernandez:** Formal analysis (equal); investigation (equal); validation (equal). **Yolanda Alvarez:** Formal analysis (equal); investigation (equal); validation (equal). **Kiril Schimmang-Alonso:** Formal analysis (equal); investigation (equal); validation (equal). **Maria Alonso:** Formal analysis (equal); investigation (equal); validation (equal). **Hannes Maier:** Formal analysis (equal); investigation (equal); validation (equal). **Matthew Anderson:** Conceptualization (equal); formal analysis (equal); investigation (equal); resources (equal); validation (equal); visualization (equal); writing – review and editing (equal). **Mark Lewandoski:** Investigation (equal); resources (equal); writing – review and editing (equal). **Thomas Schimmang:** Conceptualization (lead); formal analysis (equal); funding acquisition (equal); supervision (equal); validation (equal); writing – original draft (lead).

requirement between these *Fgfs* during otic placode induction. In contrast, inactivation of *Fgf3* and *Fgf4* in the pharyngeal region where both *Fgfs* are also co-expressed using a *Foxg1*-Cre driver did not affect development of the pharyngeal arches. However, these mutants showed reduced perinatal survival.

Conclusions: These results highlight the importance of Fgf signaling during development. In particular, different members of the Fgf family act redundantly to guarantee inner ear formation and embryonic survival.

Keywords

deafness; embryonic survival; fibroblast growth factor; hearing loss; inner ear; otic induction

1 | INTRODUCTION

Fibroblast growth factors comprise a large gene family of 22 ligands. Fgf ligands fall into three functional groups: FGF homologous factors, endocrine Fgfs, and canonical Fgfs. The latter group contains Fgfs that play key roles for organ formation during embryonic development. These essential functions are often carried out between multiple Fgf members, which act in redundancy.[1]

During inner ear induction *Fgf3*, which is prominently expressed in the developing hindbrain neighboring the otic placode (Figure 1A,B), acts in redundancy with *Fgf8* and *Fgf10*, which are found in the neighboring endoderm and mesoderm.[2] On the other hand, *Fgf3* single mutants show either normal otic development or inner ear defects during later embryogenesis and adulthood with a variable penetrance and expressivity.[3–5] Moreover, lack of *Fgf3* is associated with reduced survival during embryogenesis or early postnatal development.[4–6]

Fgf3 forms part of a gene cluster comprising *Fgf3*, *Fgf4*, and *Fgf15* (Figure 1I).[7] *Fgf4* lies in close proximity to *Fgf3* and inactivation of the former interferes with early embryonic survival.[8] *Fgf4* is co-expressed with *Fgf3* in the otic placode (Figure 1A, C,E,G) and the neighboring surface ectoderm that overlies the pharyngeal region (Figure 1B,D,F,H) but their redundant requirement during development could so far not been addressed because of their close proximity within the genome, which leads to an extremely low frequency of interallelic crossover of the existing mutant alleles. The recent generation of *Fgf3*/*Fgf4 cis* mice allows conditional inactivation of *Fgf4* on a *Fgf3* null mutant background and therefore permits the analysis of redundant functions between both of these *Fgfs*.[6] In the present study, we show that replacement of the *Fgf3* coding region by a *neomycin* resistance gene leads to an increased penetrance of inner ear defects and reduced embryonic survival. This was accompanied by reduced expression of the neighboring *Fgf4* gene in some of the mutant embryos. Conditional inactivation of *Fgf4* on an *Fgf3* null background in domains where it is co-expressed with *Fgf3* revealed redundancy between both *Fgfs* for formation of the otic placode but not during development of the pharyngeal arches. However, inactivation of *Fgf3* and *Fgf4* within this domain is likely to underlie the reduced survival of these mutants and of single *Fgf3* mutant mice.

2 | RESULTS AND DISCUSSION

Previous analysis of *Fgf3* mutant lines revealed a reduced postnatal survival of homozygous mutants (10% vs the expected 25% for heterozygous crosses) accompanied by an inner ear phenotype with incomplete penetrance (58%) and variable expressivity.[4,5] In contrast, we previously reported the generation of *Fgf3* null mutants in which all coding exons had been deleted and which lacked an inner ear phenotype.[3] These mice only showed a slightly reduced survival of homozygous knockouts (20% vs the expected 25% for heterozygous crosses) (Figure 2A).

During the course of our studies, we also examined an *Fgf3* mutant line in which the *Fgf3* coding exons had been replaced by a *neomycin* (*neo*) resistance gene. In this case, we observed a more severely reduced survival of homozygotes of 10% at weaning (Figure 2A), similar to that observed for other *Fgf3* mutant lines.[4,5] Moreover, we observed inner ear defects with characteristics similar to those reported for other *Fgf3* mutant lines in 12% of the homozygotes on a mixed genetic background. Upon back-crossing onto the B6 background, 41% of homozygous $Fgf3^{neo/neo}$ mutants showed a mutant inner ear phenotype, with a frequency similar to that reported for other *Fgf3* mouse mutants.[4] This included elevated auditory thresholds compared to wild-type and heterozygous control animals (Figure 2B). At the otic vesicle stage, mutants lacked the endolymphatic duct (Figure 2C,D). Paint-filled adult inner ears revealed abnormal formation of the cochlea and in the vestibular system the posterior canal failed to resorb and the lateral canal was missing (Figure 2E,F). Histological sections through the cochlea revealed a normal gross morphology and formation of the sensory epithelium in controls (Figure 2G,H). In contrast, homozygous $Fgf3^{neo/neo}$ mutants showed an abnormal cochlear chamber and sensory epithelium (Figure 2I,J). In the vestibular system of these mutants, we observed severely reduced sized ampullary cristae and utricular maculae (Figure 2K,L).

During embryogenesis, we observed a reduction of embryonic survival of 20% vs the expected 25% in homozygous $Fgf3^{neo/neo}$ mutants (n = 18/90). Moreover, examination throughout embryonic development of $Fgf3^{neo/neo}$ mutants revealed the presence of dead embryos around E11 with apparent craniofacial abnormalities, which may correspond to $Fgf3^{neo/neo}$ mutants (Figure 3A,B). One of the reasons for the reduced embryonic survival of $Fgf3^{neo/neo}$ may be that the *neo* gene present in the *Fgf3* locus interferes with the expression of neighboring genes. *Fgf3* forms part of the *Fgf3/Fgf4/Fgf15* gene cluster in which *Fgf4* lies only 18kB away from *Fgf3* (Figure 1E) and has been shown to be essential for embryonic survival.[8] We therefore monitored potential changes of *Fgf4* expression in $Fgf3^{neo/neo}$ mutants between E8 to E10 prior to the appearance of craniofacial abnormalities. Next to the otic placode, *Fgf4* is expressed in the tail bud and later on in the pharyngeal arches during these stages (Figure 1C,D).[9,10] We observed that *Fgf4* expression was reduced in the pharyngeal arch region in a subset of $Fgf3^{neo/neo}$ mutants (n = 2/6) (Figure 3C).

Since *Fgf4* was reduced in the pharyngeal arches of a subset of $Fgf3^{neo/neo}$ mutant embryos that may account for their increased lethality, we examined a potential redundancy between *Fgf3* and *Fgf4* by creating *Fgf3/Fgf4* double mutants. To do so, we took advantage of the *Fgf3/Fgf4* cis line, which allows conditional inactivation of *Fgf4* on a *Fgf3* null

background.[6] To conditionally inactivate *Fgf4*, we used the *Foxg1*Cre driver, which deletes floxed alleles in the ectoderm and endoderm of pharyngeal arches.[11] *Foxg1*-Cre-*Fgf3*$^{\Delta/\Delta}$/*Fgf4*$^{flox/flox}$ mouse mutants showed normal development of pharyngeal arches as revealed by hybridization with a *Dlx5* riboprobe (Figure 3D,E). However, at birth no live *Foxg1*-Cre-*Fgf3*$^{\Delta/\Delta}$/*Fgf4*$^{flox/flox}$ newborns were observed indicating perinatal lethality of these mutants (n = 0/22).

Next we focused on potential defects caused by the loss of *Fgfs* during inner ear development and first examined the effects of loss of *Fgf4*. Conditional inactivation of *Fgf4* using the *Foxg1*Cre line revealed normal formation of the otic vesicle including the endolymphatic duct, which is typically lost in *Fgf3* mutant lines with an inner ear phenotype (Figure 4A,B).[4,5] Likewise, mouse mutants in which *Fgf4* has been inactivated in the inner ear by the *Pax2*-Cre driver[12] have been reported to lack inner ear defects.

To explore redundancy between *Fgf3* and *Fgf4* during inner ear development, we used the *Fgf3/Fgf4* cis line in combination with the *Pax2*-Cre driver. However, given that the insertion of a *neomycin* resistance selection cassette into *Fgf3* can reduce *Fgf4* expression (Figure 3C), we first determined whether the inserted *hygromycin* resistance selection cassette within *Fgf3* in *Fgf3/Fgf4* cis embryos likewise affects otic placode specific expression of the nearby *Fgf4flox* allele. To do this, we measured *Fgf4* mRNAs fluorescently labeled by hybridization chain reaction (HCR).[13] We measured this HCR signal within an Imaris-based volume[14] of the otic placode-specific *Fgf4* expression domain. We found that *Fgf4* mRNA levels per volume of *Fgf4*-expressing tissue were reduced to 90% of wild-type expression in *Fgf3/Fgf4* cis heterozygotes and 83% in homozygotes (Figure 5A–D). However, the *Fgf4* expression domain volume itself was also reduced, compared to controls, to 73% in *Fgf3/Fgf4* cis heterozygotes and 55% in homozygotes. We surmise this reduction is due to a loss of *Fgf3* function. This reduction of volume multiples the reduction of per se *Fgf4* mRNA levels, producing an effective reduction of 45% in *Fgf3/Fgf4* cis homozygotes, compared to wild-type littermate controls (eg, reduction in mRNA levels multiplied by a reduction in tissue). Therefore, overall the loss of *Fgf4* expression in the *Fgf3/Fgf4* cis homozygotes is largely due to the reduced size of the placode caused by the absence of *Fgf3* rather than the insertional effect of the *hygromycin* resistance selection cassette in the *Fgf3* locus.

Mouse mutants with a *Pax2*-Cre-mediated inactivation of *Fgf4* within an *Fgf3* null homozygous background showed loss of *Pax2* expression, which labels the otic placode (Figure 4C,D) and no otic tissue at the otic vesicle stage as revealed by labeling with a *Dlx5* riboprobe (Figure 4E–G). Of note, this analysis reveals that the reduced *Fgf4* mRNA levels in *Fgf3/Fgf4* cis homozygotes (Figure 3C), suffices to maintain otic tissue, albeit smaller than controls and without an endolymphatic duct (compare Figure 4F with E), indicating an independent requirement of *Fgf3* in endolymphatic duct formation. Identical results were obtained when using the *Fgf3/Fgf4* cis line in combination with the *Foxg1*-Cre driver, which also drives expression throughout inner ear formation[11] (data not shown).

The *Fgf3/Fgf4/Fgf15* cluster is well known for its high probability to recombine due to insertional mutagenesis.[15] Interestingly, this has not only been confirmed in the context of

cancer but also for craniofacial development.[16] In this case, insertion of a retrovirus between the *Fgf3* and *Fgf4* coding region has been demonstrated to cause ectopic misexpression of both *Fgfs*.

Interestingly, in embryos that lack both *Fgf3* and *Fgf10* and fail to induce the inner ear, *Fgf4* expression is absent in the dorsal surface ectoderm, which usually gives rise to the otic placode.[10] This may indicate that its expression is essential for inner ear induction. However, as shown in the present study, inactivation of *Fgf4* expression in the otic placode by its own did not affect inner ear induction confirming that none of the group of Fgfs, comprising *Fgf3*, *Fgf4*, *Fgf8*, and *Fgf10*, is uniquely required for this process. Finally, although *Fgf15* is not expressed in tissues directly involved in inner ear induction and its inactivation confirmed that it is not required for formation of the otic vesicle,[17] its co-deletion together with other *Fgfs* may still reveal further redundancies between different Fgf family members during embryonic development. While we observed redundant requirement for *Fgf3* and *Fgf4* during inner ear induction, this was not the case for craniofacial development. Co-deletion of additional *Fgfs* expressed in pharyngeal arches, such as *Fgf8*, may unveil potential further redundancies with *Fgf3* and *Fgf4* in this domain.[18]

Although we could not confirm a lack of embryonic survival at around E11, such as observed in $Fgf3^{neo/neo}$ mutants, perinatal survival was clearly compromised in *Foxg1*-Cre-*Fgf3/Fgf4* mutants. Stochastic loss of *Fgf4* expression such as that observed in the $Fgf3^{neo/neo}$ mutant may therefore also influence the survival of other *Fgf3* mutants.[4,5] Additionally, background modifiers apparently influence the survival and expressivity of the inner ear phenotype of *Fgf3* mutants. Genetic changes within the *Fgf3/Fgf4/Fgf15* cluster are thus prone to cause phenotypes with a variable penetrance and expressivity. Availability of tools such as the *Fgf3/Fgf4* cis line is therefore useful to further explore the link between these genetic changes and the phenotypes caused by them.

3 | EXPERIMENTAL PROCEDURES

3.1 | Transgenic mice and targeted mouse lines

Generation and genotyping of mice carrying the $Fgf3^{\Delta}$ and $Fgf3^{neo}$ alleles,[3] *Fgf3/Fgf4 cis allele*,[6] *Pax2*-Cre,[12] and the *Foxg1*-Cre drivers[11] have been described previously. Experiments conformed to the institutional and national regulatory standards concerning animal welfare.

3.2 | Histology, β-galactosidase staining, RNA in situ hybridization and paint-fillings of inner ears

Preparation and staining of histological sections, RNA whole-mount in situ hybridization,[3] and paint-filling of inner ears was performed as described previously.[19]

3.3 | Auditory brain stem responses

Auditory click-evoked brainstem responses (ABR) were used to determine hearing thresholds in anesthetized (xylazin hydrochloride 16 mg/kg body weight and S-ketamin hydrochloride 60 mg/kg body weight) animals between 6 and 8 weeks of age. Alternating

acoustic stimuli were applied monaurally at a rate of 21/s and bioelectric responses were averaged 400–2000 times. Stimulus intensities were varied from 117 dB peak equivalent SPL (pe dB SPL) in increments of 20 dB except near threshold where 5 dB steps were used. Thresholds as defined by the lowest level to generate a reproducible ABR wave were determined visually from averaged responses blinded, without knowledge of the genotype.

ABR thresholds in all groups were normally distributed (Shapiro-Wilk) and all statistical comparisons between groups were performed using the non-paired *t* test. As no statistical significant difference between wild-type (53.7 ± 4.8 pe dB SPL; N = 4) and *Fgf3*$^{neo/+}$ (53.7 ± 4.1 pe dB SPL; N = 6) animals was found (54.5 ± 4.2 pe dB SPL; N = 6), the pooled group was used as controls. Thresholds of *Fgf3*$^{neo/neo}$ animals (88.6 ± 21.3 pe dB SPL; N = 16) were found to be significantly different from controls (two-tailed; $P < .001$).

3.4 | Hybridization chain reaction (HCR) whole mount in situ and Imaris modeling

HCR and Imaris modeling were performed as previously described.[14] Alexafluor-546 hairpins were used to label *Fgf4* mRNA bound probes; hairpins and v3.0 probes were purchased from Molecular Instruments, Inc. Confocal images were captured on a Nikon A1 laser scanning confocal using a 10x plan apo lambda objective (NA: 0.4). Images were processed in Imaris (Bitplane) using a conservative baseline subtraction threshold of 100 to eliminate tissue autofluorescence and non-specific probe binding. The *Fgf4* otic placode expression domain was modeled using Imaris Surface objects, generated with a surface detail of 3.43 μm and threshold of 100.

ACKNOWLEDGMENTS

This work was supported by MinEco (BFU2004-00860/BFI) and Programa Estratégico Instituto de Biología y Genética Molecular (IBGM), Escalera de Excelencia, Junta de Castilla y León (Ref. CLU-2019-02) and Programa Estratégico Instituto de Biología y Genética Molecular (IBGM), Junta de Castilla y León (Ref. CCVC8485).

REFERENCES

1. Ornitz DM, Itoh N. The fibroblast growth factor signaling pathway. Wiley Interdiscip Rev Dev Biol. 2015;4(3):215–266. 10.1002/wdev.176 [PubMed: 25772309]
2. Expression Schimmang T. and functions of FGF ligands during early otic development. Int J Dev Biol. 2007;51(6–7):473–481. 10.1387/ijdb.072334ts [PubMed: 17891710]
3. Alvarez Y, Alonso MT, Vendrell V, et al. Requirements for FGF3 and FGF10 during inner ear formation. Development. 2003;130(25):6329–6338. 10.1242/dev.00881 [PubMed: 14623822]
4. Hatch EP, Noyes CA, Wang X, Wright TJ, Mansour SL. Fgf3 is required for dorsal patterning and morphogenesis of the inner ear epithelium. Development. 2007;134(20):3615–3625. 10.1242/dev.006627 [PubMed: 17855431]
5. Mansour SL, Goddard JM, Capecchi MR. Mice homozygous for a targeted disruption of the proto-oncogene int-2 have developmental defects in the tail and inner ear. Development. 1993;117(1):13–28. [PubMed: 8223243]
6. Anderson MJ, Southon E, Tessarollo L, Lewandoski M. Fgf3-Fgf4-cis: a new mouse line for studying Fgf functions during mouse development. Genesis. 2016;54(2):91–98. 10.1002/dvg.22913 [PubMed: 26666435]
7. Ornitz DM, Itoh N. Fibroblast growth factors. Genome Biol. 2001;2(3):REVIEWS3005. 10.1186/gb-2001-2-3-reviews3005 [PubMed: 11276432]

8. Feldman B, Poueymirou W, Papaioannou VE, DeChiara TM, Goldfarb M. Requirement of FGF-4 for postimplantation mouse development. Science. 1995;267(5195):246–249. 10.1126/science.7809630 [PubMed: 7809630]
9. Wright TJ, Hatch EP, Karabagli H, Karabagli P, Schoenwolf GC, Mansour SL. Expression of mouse fibroblast growth factor and fibroblast growth factor receptor genes during early inner ear development. Dev Dyn. 2003;228(2):267–272. 10.1002/dvdy.10362 [PubMed: 14517998]
10. Urness LD, Paxton CN, Wang X, Schoenwolf GC, Mansour SL. FGF signaling regulates otic placode induction and refinement by controlling both ectodermal target genes and hindbrain Wnt8a. Dev Biol. 2010;340(2):595–604. 10.1016/j.ydbio.2010.02.016 [PubMed: 20171206]
11. Hebert JM, McConnell SK. Targeting of cre to the Foxg1 (BF-1) locus mediates loxP recombination in the telencephalon and other developing head structures. Dev Biol. 2000;222(2):296–306. 10.1006/dbio.2000.9732 [PubMed: 10837119]
12. Ohyama T, Groves AK. Generation of Pax2-Cre mice by modification of a Pax2 bacterial artificial chromosome. Genesis. 2004;38(4):195–199. 10.1002/gene.20017 [PubMed: 15083520]
13. Trivedi V, Choi HMT, Fraser SE, Pierce NA. Multidimensional quantitative analysis of mRNA expression within intact vertebrate embryos. Development. 2018;145(1):156869. 10.1242/dev.156869
14. Anderson MJ, Magidson V, Kageyama R, Lewandoski M. Fgf4 maintains Hes7 levels critical for normal somite segmentation clock function. Elife. 2020;9:55608. 10.7554/eLife.55608
15. Katoh M WNT and FGF gene clusters (review). Int J Oncol. 2002;21(6):1269–1273. [PubMed: 12429977]
16. Carlton MB, Colledge WH, Evans MJ. Crouzon-like craniofacial dysmorphology in the mouse is caused by an insertional mutation at the Fgf3/Fgf4 locus. Dev Dyn. 1998;212(2):242–249. 10.1002/(SICI)1097-0177(199806)212:2<242::AID-AJA8>3.0.CO;2-H. [PubMed: 9626498]
17. Wright TJ, Ladher R, McWhirter J, Murre C, Schoenwolf GC, Mansour SL. Mouse FGF15 is the ortholog of human and chick FGF19, but is not uniquely required for otic induction. Dev Biol. 2004;269(1):264–275. 10.1016/j.ydbio.2004.02.003 [PubMed: 15081372]
18. Jackson A, Kasah S, Mansour SL, Morrow B, Basson MA. Endoderm-specific deletion of Tbx1 reveals an FGF-independent role for Tbx1 in pharyngeal apparatus morphogenesis. Dev Dyn. 2014;243(9):1143–1151. 10.1002/dvdy.24147 [PubMed: 24812002]
19. Morsli H, Choo D, Ryan A, Johnson R, Wu DK. Development of the mouse inner ear and origin of its sensory organs. J Neurosci. 1998;18(9):3327–3335. [PubMed: 9547240]

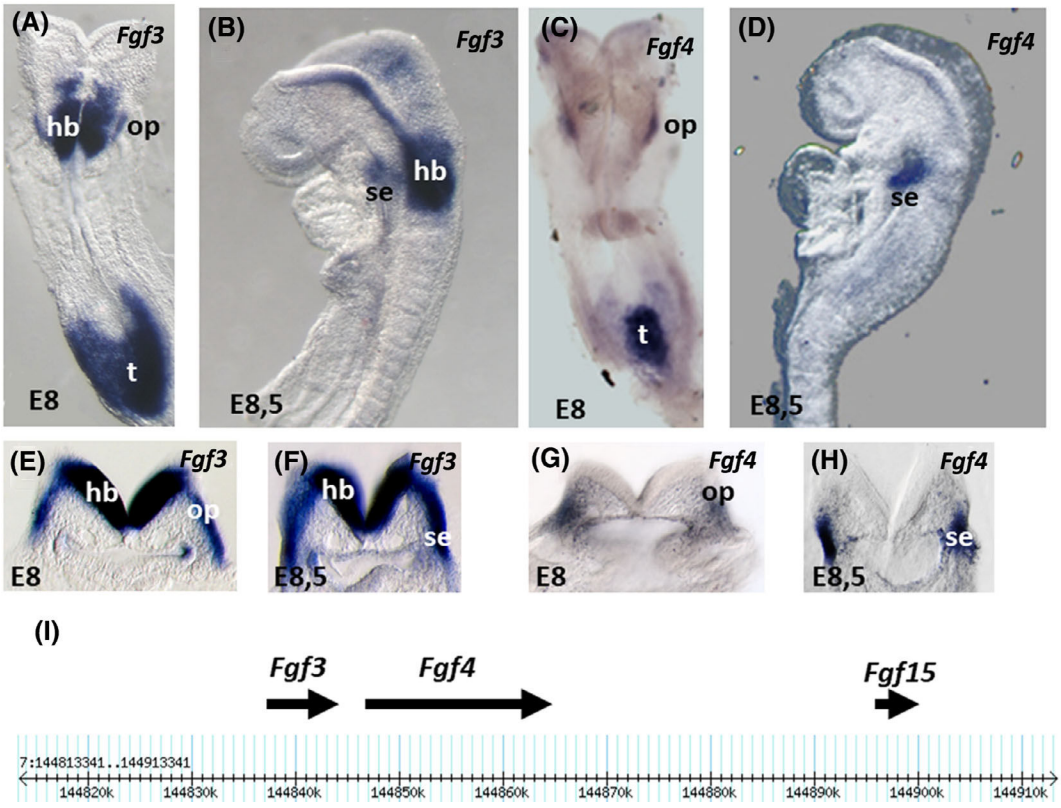

FIGURE 1.

Expression sites for *Fgf3* and *Fgf4* during early development and the *Fgf3/Fgf4/Fgf15* gene cluster in mouse. Expression of *Fgf3* and *Fgf4* at embryonic day 8 (E8) and E8,5 shown by whole mount hybridisation (A-D) and on sections (E-H). (A,B,E,F) *Fgf3* expression is observed in the hindbrain (hb), tailbud (t), otic placode (op) and the neighboring surface ectoderm (se), which overlies the pharyngeal region. (C,D,G,H) *Fgf4* expression is detected in the tail bud, otic placode and the neighboring surface ectoderm. (I) Scheme of the *Fgf3/Fgf4/Fgf15* gene cluster on mouse chromosome 7 (from MGI)

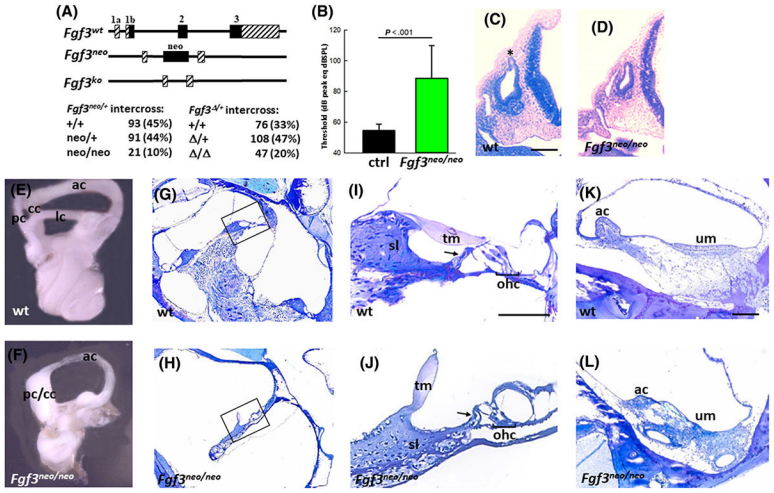

FIGURE 2.

Inner ear defects in *Fgf3*^{neo} mutant mice in which its coding region has been replaced by a *neomycin* resistance gene. (A) Top: Scheme of the *Fgf3* locus and the generation of alleles carrying a *neomycin* resistance gene (*neo*) or a null allele (*Δ*). Bottom: Genotypes at weaning of *Fgf3*$^{+/neo}$ and *Fgf3*$^{+/Δ}$ intercrosses. Numbers and percentage of total (in parentheses) for wild-type (+/+), heterozygous (+/*neo* or +/*Δ*) and homozygous (*neo*/*neo* or *Δ*/*Δ*) B) Auditory brainstem response thresholds (in decibels sound pressure level) of controls and *Fgf3*$^{neo/neo}$ mutants. (C,D) Sections through the otic vesicle at embryonic day 10 reveals absence of the endolymphatic duct (indicated by an asterisk) in *Fgf3*$^{neo/neo}$ mutants. (E,F) Paint-filled inner ears of the bony labyrinth of a wild-type (wt) and an *Fgf3*$^{neo/neo}$ mutant. Note the absence of the lateral canal (lc) and the failure of the posterior canal (pc) to resorb. Low (G,H) and high (I,J) magnification views of toluidin blue-stained sections through the cochlea of adult wild-type and *Fgf3*$^{neo/neo}$ mutants. The positions of the inner and outer hair cells (ohc) are indicated by an arrow and a bracket, respectively. (K,L) Sections through vestibular system reveal reduced sized ampullary cristae (ac) and utricular maculae (um) in the mutants (K,L) compared to wild types. Scale bars: 200 μm in C; 50 μm in I,K. ac, anterior canal; cc, common crus; sl, spiral lamina; tm, tectorial membrane; oC, organ of Corti

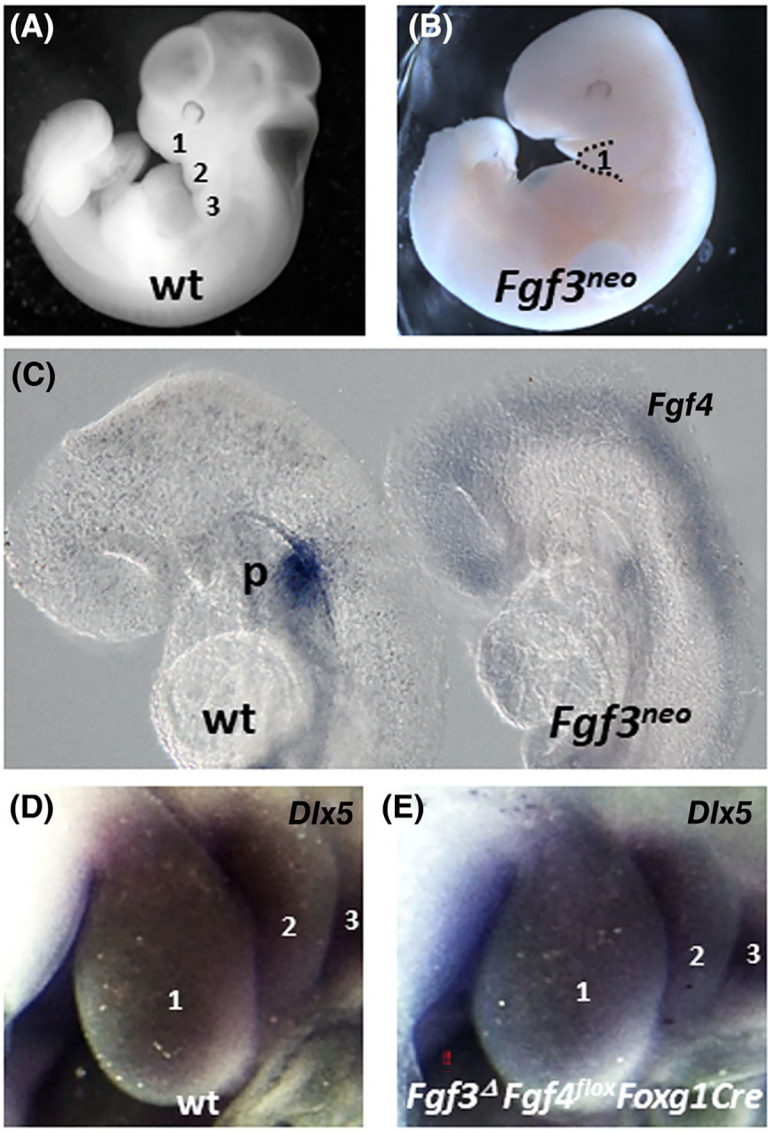

FIGURE 3.

Fgf4 expression and development of pharyngeal arches in *Fgf* mutants. (A,B) Phenotype of wt and $Fgf3^{neo/neo}$ mutants at E11. Pharyngeal arches are indicated by numbers. Note the craniofacial defects in $Fgf3^{neo/neo}$ mutants. In the mutant, the circumference of the first pharyngeal arch is indicated by stippled lines. (C) *Fgf4* expression in the pharyngeal arches (p) of wild-type and $Fgf3^{neo/neo}$ mutants. (D,E) Normal formation of pharyngeal arches labeled with a *Dlx5* riboprobe is observed in wt and *Foxg1*-Cre-$Fgf3^{\Delta/\Delta}/Fgf4^{flox/flox}$ mutants

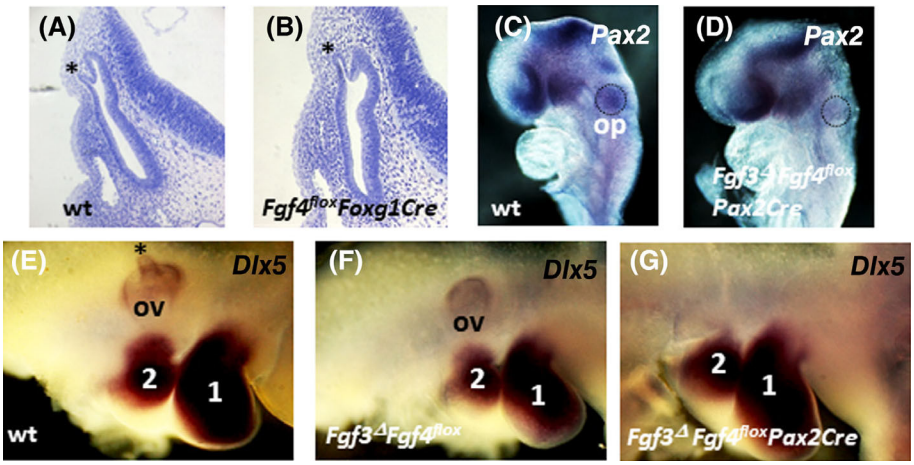

FIGURE 4.

Inner ear induction in *Fgf4* and *Fgf3/Fgf4* mutants. (A,B) Toluidin blue stained sections through the otic vesicles of wild-type (wt) and *Foxg1*Cre-*Fgf4*$^{flox/flox}$ mutants at E10. The endolymphatic duct is labeled with an asterisk. (C-G) Whole-mount hybridisation of embryos with the indicated genotypes labeled with a *Pax2* at E8 (C,D) and a *Dlx5* probe at E10,5 (E-G). Note the absence of *Pax2* staining in the otic placode (op, indicated by dotted lines) and of otic tissue in *Pax2*-Cre-*Fgf3*$^{\Delta/\Delta}$/*Fgf4*$^{flox/flox}$ mutants. *Fgf3*$^{\Delta/\Delta}$/*Fgf4*$^{flox/flox}$ mutant otic vesicles (ov) lack the endolymphatic duct (labeled with an asterisk)

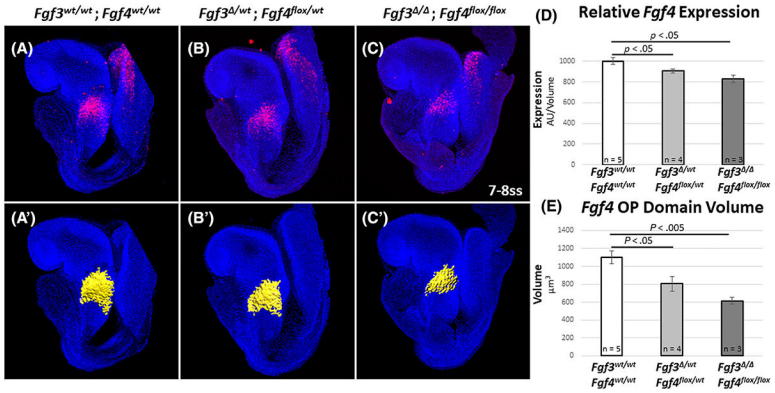

FIGURE 5.

Quantification of *Fgf4* expression in the otic placode of $Fgf3^{\Delta}$; $Fgf4^{flox}$ embryos. (A-C) HCR whole mount in situ analysis of *Fgf4* mRNA expression in 7–8 somite staged (ss) $Fgf3^{wt/wt}$; $Fgf4^{wt/wt}$, $Fgf3^{\Delta/wt}$; $Fgf4^{flox/wt}$, and $Fgf3^{\Delta/\Delta}$; $Fgf4^{flox/flox}$ littermates. (A'-C′) Imaris surface modeling of *Fgf4* expression in the otic placode in the same embryos shown in A-C. (D) Quantification of fluorescent signal from HCR labeled *Fgf4* mRNA per volume of the otic placode domain of *Fgf4* expression. Expression level values are normalized to that measured in $Fgf3^{wt/wt}Fgf4^{wt/wt}$ control littermates (set to 1.0). The *Fgf4* mRNA level within placodes of the $Fgf3^{\Delta/wt}$; $Fgf4^{flox/wt}$ mutants is 90% of controls and, within $Fgf3^{\Delta/\Delta}$; $Fgf4^{flox/flox}$, 83.0% of controls. (E) Measurement of the *Fgf4* otic placode (OP) domain volume using Imaris Surface modeling. The OP-specific *Fgf4* expression volume within $Fgf3^{\Delta/wt}$; $Fgf4^{flox/wt}$ mutants is 73% of controls, and within $Fgf3^{\Delta/\Delta}$; $Fgf4^{flox/flox}$, 55% of controls. Therefore, the effective reduction of *Fgf4* mRNA in $Fgf3^{\Delta/\Delta}$; $Fgf4^{flox/flox}$ mutants is 45% of controls. A-C′ are maximum intensity projections, lateral views, anterior to the left. Number of embryos examined are noted in panels D, E. Error bars (D, E) represent SE of the mean, significance determined by a two-tailed Students *t*-test